González-Domínguez, E.; Berlanas, C.; Gramaje, D.; Armengol Fortí, J.; Rossi, V.; Berbegal Martinez, M. (2020). Temporal dispersal patterns of Phaeomoniella chlamydospora, causal agent of Petri disease and esca, in vineyards. Plant Disease. 110(6):1216-1225. https://doi.org/10.1094/PHYTO-10-19-0400-R

Temporal dispersal patterns of *Phaeomoniella chlamydospora*, causal agent of Petri disease and esca, in vineyards

Elisa González-Domínguez†, Carmen Berlanas, David Gramaje, Josep Armengol, Vittorio Rossi, Mónica Berbegal

First author: Horta srl., Via Egidio Gorra 55, 29122 Piacenza, Italy; second and third authors: Instituto de Ciencias de la Vid y del Vino (ICVV), Consejo Superior de Investigaciones Científicas - Universidad de la Rioja - Gobierno de La Rioja, Ctra. LO-20 Salida 13, Finca La Grajera, 26071 Logroño, Spain; fourth and sixth authors: Instituto Agroforestal Mediterráneo, Universitat Politècnica de València, Camino de Vera s/n, 46022 Valencia, Spain; fifth author: Department of Sustainable Crop Production (DIPROVES), Facoltà di Scienze Agrarie, Alimentari e Ambientali, Università Cattolica del Sacro Cuore, Via Emilia Parmense, 84, 29122 Piacenza, Italy.

†Corresponding author: Elisa González-Domínguez; E-mail: e.gonzalez@horta-srl.com

ABSTRACT

Although the fungus *Phaeomoniella chlamydospora* is the most commonly detected causal agent of Petri disease and esca, two important fungal grapevine trunk diseases (GTDs), little is known about the dispersal patterns of *P. chlamydospora* inoculum. In this work, we studied the dispersal of *P. chlamydospora* airborne inoculum from 2016 to 2018 in two viticultural areas of eastern (Ontinyent) and northern (Logroño) Spain. The vineyards were monitored weekly from November to April using microscope slide traps, and *P. chlamydospora* was detected and quantified by a specific qPCR method set up in this work. The method was found to be sensitive, and a good correlation was observed between numbers of *P. chlamydospora* conidia (counted by microscope) and DNA copy numbers (quantified by qPCR). We consistently detected DNA of *P. chlamydospora* at both locations and in all seasons but in different quantities. In most cases, DNA was first detected in the last half of November, and most of the DNA was detected from December

to early April. When rain was used as a predictor of *P. chlamydospora* DNA detection in traps, false negative detections were observed, but these involved only the 4% of the total. The dispersal pattern of *P. chlamydospora* DNA over time was best described (R^2 = 0.765 and concordance correlation coefficient = 0.870) by a Gompertz equation, with time expressed as hydro-thermal (a physiological time accounting for the effects of temperature and rain). This equation could be used to predict periods with a high risk of dispersal of *P. chlamydospora*.

Keywords: grapevine trunk diseases, hydro-thermal time, real-time quantitative PCR, *Vitis vinifera*.

Petri disease and esca are grapevine trunk diseases (GTDs) that represent a serious threat to viticulture worldwide (Gramaje et al., 2018). The fungi *Phaeomoniella chlamydospora*, *Phaeoacremonium* species, and *Cadophora luteo-olivacea* are the main causal agents of Petri disease in young vineyards (Bertsch et al. 2013; Gramaje et al. 2011; Gramaje et al. 2015 and 2018). In mature vineyards, the same fungi together with *Fomitiporia mediterranea* and other basidiomycetes are associated with esca (Bertsch et al. 2013; Cloete et al. 2015; Fischer and González-García 2015).

The etiology of these GTDs is complex because grapevines can be simultaneously infected by different pathogens, and the symptoms caused by these pathogens can overlap (Gramaje et al. 2018). In brief, Petri disease is characterized by the presence of phenolic compounds in the xylem vessels of the trunk (producing dark exudates when the trunk is cut) and dark streaks in longitudinal sections (Gubler et al. 2015). Esca is characterized by the appearance of multiple discolored bands in a ‘tiger-stripe’ pattern on the foliage. Esca can also have an apoplectic form, characterized by a sudden wilting of shoots, arms or the

entire plant. Internal wood symptoms of esca include black spots in the xylem, brown to black vascular streaking, and a white to yellow soft rot in older vines (Gramaje et al. 2018).

Phaeomoniella chlamydospora is an especially important GTD pathogen because it has been associated with both Petri disease and esca, and because it is the fungus most frequently isolated from affected vines (Bertsch et al. 2013; Gubler et al. 2015). *P. chlamydospora*, which is an anamorphic member of the Family Phaeomoniellaceae in the order Phaeomoniellales of the Eurotiomycetes (Pezizomycotina, Ascomycota), has an unknown teleomorph. It produces conidia on conidiophores that arise directly from hyphae, but produces conidia also in pycnidia of a *Phoma*-like synanamorph (Crous and Gams 2000; Chen et al. 2015).

Phaeomoniella chlamydospora overwinters as pycnidia in pruning wounds, although mycelium on infected wood can also produce conidia (Baloyi et al. 2016; Edwards and Pascoe 2001; Edwards et al. 2001). From these sources, inoculum of *P. chlamydospora* is aerially dispersed (Eskalen and Gubler 2001; Quaglia et al. 2009; Larignon and Dubos 2000). *P. chlamydospora* conidia may also be dispersed by arthropods (Moyo et al. 2014) and by pruning shears (Agustí-Brisach et al. 2015). The conidia produce germ tubes that enter the plant through pruning wounds (Eskalen et al. 2007; Larignon and Dubos 2000; Serra et al. 2008), although the susceptibility of pruning wounds significantly decreases over time (Elena and Luque 2016; Eskalen et al. 2007; Larignon and Dubos 2000; Serra et al. 2008; van Niekerk et al. 2011). *P. chlamydospora* can also be disseminated with grapevine propagation material (Fourie and Halleen 2002; Halleen et al. 2003; Whiteman et al. 2007), and is commonly detected in grafted commercial plants (Bertelli et al. 1998; Giménez-Jaime et al. 2006). In grapevine nurseries, PCR analyses have confirmed the presence of *P. chlamydospora* inoculum in hydration tanks, on grafting tools, and on the

substrates used for callusing (Aroca et al. 2010; Edwards et al. 2007; Retief et al. 2006; Ridgway et al. 2002).

It is widely accepted that the infection of pruning wounds by aerial inoculum is the main infection pathway for GTDs (Rolshausen et al. 2010, van Niekerk et al. 2011), but little is known about the dispersal patterns of *P. chlamydospora* conidia. Early studies showed that conidia of *P. chlamydospora* were dispersed throughout the year in France and California (Eskalen and Gubler 2001; Larignon and Dubos 2000), but conidia were trapped only from March to December in vineyards in Italy (Quaglia et al. 2009). In California and Italy, dissemination of conidia occurred mainly during or following rain events (Eskalen and Gubler 2001; Quaglia et al. 2009). These studies, however, provided little information about the effects of environmental conditions on the dispersal dynamics of *P. chlamydospora* conidia. The latter information is essential for identifying periods with a high risk of spore dispersal and for adopting efficient management strategies.

Past studies of the dispersal of *P. chlamydospora* conidia were based on classical microbiological methods, such as the microscopic counting of spores from spore traps or the counting of fungal colonies from spore traps on culture media (Eskalen and Gubler 2001; Larignon and Dubos 2000; Quaglia et al. 2009; van Niekerk et al. 2010). These procedures are time-consuming and limited in accuracy and sensitivity due to the small size of the spores and their similarity with the conidia of *Phaeoacremonium* species and *C. luteo-olivacea* (Crous and Gams 2000; Gramaje et al. 2011, 2015). Real-time quantitative PCR (qPCR) combines specificity with accurate and sensitive measurement of DNA copy number. Several qPCR methods have been developed for *P. chlamydospora* using different chemistries and target regions (Edwards et al. 2007; Martín et al. 2012; Overton et al. 2004; Pouzoulet et al. 2013), but have not been applied to detect and quantify the pathogen's conidia in spore traps.

The aim of this study was to analyze the dynamics of *P. chlamydospora* airborne inoculum in vineyards in relation to weather conditions. For this purpose, we set up a rapid, specific, and highly sensitive qPCR-based method for detection of *P. chlamydospora* DNA. The study had four specific objectives: (i) to develop a simple trapping system compatible with the DNA-based method for detection and quantification of *P. chlamydospora* airborne inoculum, (ii) to study the release dynamics of *P. chlamydospora* in two wine-producing regions of Spain over a 3-year period, (iii) to investigate the relationships between the release dynamics and weather conditions, and (iv) to develop equations for predicting the dispersal patterns of *P. clamydospora* in vineyards.

MATERIALS AND METHODS

Laboratory samples. Total DNA of a representative *P. chlamydospora* isolate (Pch184) (Tello et al. 2010) obtained from the culture collection of the Instituto Agroforestal Mediterráneo-Universitat Politècnica de València (IAM-UPV) (Spain) was extracted with the EZNA Plant Miniprep Kit (Omega Bio-Tek, Norcross, GA). Before DNA extraction, the sample was homogenized in 2-ml tubes containing 600 µl of P1 buffer (provided in the kit) and three 3-mm-diameter tungsten carbide beads (Qiagen, Hilden, Germany); the beads facilitated the rupture of mycelia and conidia when the preparation was subjected to vibration in a FastPrep® (MP Biomedicals, Santa Ana, CA, USA) at 50 Hz for 30 s. The concentration (ng/µl) of the genomic DNA (gDNA) obtained was quantified with the Qubit Fluorometric Quantitation kit (Life Technologies, Carlsbad, CA, USA). Seven 1:10-fold serial dilutions of gDNA were prepared.

For preparation of *P. chlamydospora* conidial suspensions, the fungus was grown on 9-cm Petri dishes in the dark on potato dextrose agar (PDA) for 3 weeks at 25 ºC. Each

of three suspensions (designated A, B, and C) was obtained by scraping the mycelia on a Petri dish with 20 ml of sterile water. After the suspensions were passed through cheesecloth and the volume was increased to 200 ml, seven 10-fold dilutions were made from suspensions and a total of 500 µl of each dilution was evenly distributed on a 48-mm-long siliconed (Lanzoni S.r.l., Bologna, Italy) Melinex® plastic tape (Burkard Scientific Ltd., Uxbridge, UK) on a glass microscope slide (25 × 76 mm). Concentration of the three conidial suspensions dilution series was determined by microscopic counts using a haemocytometer. Sensitivity of this methodology allowed to calculate concentrations until the third dilution and measurements for each suspension were repeated three times. A negative control tape was also included in the assay in which 500 µl of sterile water rather than a conidial suspension was distributed on the tape. The tapes were dried for 24 h before DNA was extracted as described below. Dilution series prepared from suspensions A and B were used to determine the relationship between *P. chlamydospora* conidia counts determined by microscopy and DNA copy number determined by qPCR. Conidial suspension C was used to determine DNA extraction efficiency, i.e., the relationship between *P. chlamydospora* conidia counts determined by microscopy and DNA quantity as determined by qPCR as described below.

Field samples and spore trapping. Vineyards with a history of esca symptoms and positive isolation of *P. chlamydospora*, located in Ontinyent (Alicante region, southeastern Spain) and Logroño (La Rioja region, northern Spain) were selected for the study. Two vineyards were located in Ontinyent; one was planted with cv. 'Malvasía', was 30 years old, and was sampled during the 2015/2016 growing season; the second was planted with cv. 'Monastrell', was 20 years old, and was sampled during the 2016/2017 growing season. In Logroño, two vineyards that were less than 500 m apart were sampled;

one was planted with cv. 'Tempranillo', was 42 years old, and was sampled during the 2015/2016 growing season; the second was planted with cv. 'Tempranillo', was 39 years old, and was sampled during the 2016/2017 growing season and also during the 2017/2018 growing season. All four vineyards had a traditional low-density, head-trained (bush vines) system, and were managed following the common viticulture practices of each region.

Airborne particles from both locations were collected using glass microscope slide traps. Each trap consisted of a 52-mm-long piece of silicone-coated Melinex® tape set to a slide and sticked on the 2 mm side margins. The slide was attached to a structure near the trunk of a grapevine and at a 45º angle relative to the soil surface. Five traps (at least 10 m apart) were deployed in each vineyard and were replaced weekly. Traps were first deployed on 21 November 2015 and 12 November 2015 in Ontinyent, and on 4 November 2015, 2 November 2016, and 1 November 2017 in Logroño; in all cases, trapping ended on 5 May of the following year.

In both locations, standard weather stations (Spectrum Technologies, Inc., Plainfield, IL, USA) were installed, with sensors at 1 m above the ground. The stations provided an hourly record of air temperature (T, ºC), relative humidity (RH, %), rainfall (R, mm), and leaf wetness (W, min).

DNA extraction from laboratory and field samples. Three commercial DNA extraction kits were evaluated for their suitability for the extraction of DNA from microscope slide traps: the EZNA Plant Miniprep kit (Omega Bio-Tek, Norcross, GA), the Power Plant kit (Qiagen), and the Power Soil kit (Qiagen). In a preliminary study, these kits were compared using non-exposed and field-exposed tapes in spore traps that were artificially inoculated with a *P. chlamydospora* conidial suspension in the laboratory as described earlier. The tape from each trap was cut into six equal fragments that were placed

in a 2-ml tube. Each tube contained the first buffer designated for each kit and about 100 g of 0.5-mm-diameter BashingBeads, which were collected from ZR BashingBeadTM Lysis Tubes (Zymo Research, CA, USA) and which were added to facilitate the rupture of the conidia by vibration in a Fastprep® at 50 Hz for 30 s. DNA extractions were completed following the manufacturer's protocol provided with each kit. Three replicate tapes were extracted for each combination of dilution and kit. DNA integrity was evaluated by electrophoresis in a 1.5% agarose gel with 1× TAE buffer. Gels were stained with 1× GelRed™ nucleic acid gel stain (Biotium, Hayward, CA, USA) and visualized under UV light. Concentrations of DNA for all samples were determined using a Nanodrop 2000 spectrophotometer (Thermo Fisher Scientific, Loughbrough, UK). Of the three DNA extraction kits, the EZNA Plant Miniprep and Power Plant kits provided more consistent DNA yields than the Power Soil kit (*data not shown*). Because it was the easier to use than the Power Plant kit, the EZNA kit was used for all experiments.

For laboratory samples (tapes treated with conidial suspensions prepared in the laboratory), tapes were cut and DNA was extracted with the EZNA kit. The DNA extraction product from 500 µl of conidial suspension C placed in the tape was subjected to seven 10-fold dilutions. These DNA samples and those obtained from the dilutions placed directly in the tapes were compared to determine DNA extraction efficiency.

For field samples (tapes that were placed in the vineyards), the 2-mm margins of the long sides of the tape that were fixed to the slide in the trap were removed; this did not change the total capturing surface of the tape. The tapes were subsequently processed for DNA extraction as previously described for laboratory samples. Extracted DNA was kept at -20ºC until it was subjected to PCR amplification.

Construction of the standard curve. A standard curve for the quantification of *P. chlamydospora* was constructed using a chemically-synthesized single copy of a 360-bp internal fragment of the 18S ribosomal RNA gene that included the annealing sites for Pch1 and Pch2 (Tegli et al. 2000). The 500-ng lyophilised Pch gBlocks® (Integrated DNA Technologies Inc., Skokie, IL, USA) was resuspended in 50 µl of TE Buffer (Tris and EDTA, pH 8.0; Sigma Aldrich, St. Louis, MI, USA) following the manufacturer's recommendation to obtain a final concentration of 10 ng/µl.

The total copy number of the Pch gBlocks® was determined using the following formula (Lee et al. 2006): No. of copies = (6.02×10^{23} (copy/mol) × DNA amount (g))/(DNA length (bp) × 660 (g/mol/dp)). The 10 ng/µl stock solution of Pch gBlocks® was calculated at 2.5×10^{10} copies. A 10-fold dilution series from 2.5×10^{9} to 2.5 copies was prepared and used to develop a standard curve with the qPCR conditions described in detail in the next section. Each 25-µl first-round nested-PCR reaction contained 12.5 µl of Premix Ex Taq™ (2x) (Takara Bio Inc., Shiga, Japan), 0.4 µM of each primer, and 2 µl of each standard solution (5×10^{9} to 5 copies per reaction). First-round reactions were performed in a Veriti Thermalcycler (Applied Biosystems, Foster City, CA, USA).

The quantification cycle (Cq) value for each Pch gBlocks® standard sample was calculated and analyzed using Rotor-Gene Q Series software (version 2.3.1) to generate a standard curve. The number of copies for each Pch gBlocks® standard dilution was plotted against the Cq value, and the resulting regression equations were used to quantify the number of copies of the target gene in the unknown samples. The limit of detection and sensitivity of the qPCR was determined using Pch gBlock standards and gDNA as templates. The following gDNA concentrations obtained from *P. chlamydospora* isolate (Pch184) were used as templates: 3.7×10^{7}, 3.7×10^{6}, 3.7×10^{5}, 3.7×10^{4}, 3.7×10^{3}, 370, 37, and 3.7 fg/reaction. These gDNA samples were analyzed by qPCR with Pch gBlocks® as

228 standards using four replicates in two independent assays following the conditions
229 described below. The nomenclature for interpreting all qPCR results followed the MIQE
230 guidelines as described by Bustin et al. (2009).
231
232 **Quantitative PCR analysis of samples.** Because low concentrations of fungal
233 DNA were expected in the samples collected in vineyards, a nested PCR that included a
234 conventional PCR for the first round and a real-time PCR for the second round was used.
235 The number of cycles in which the DNA of the most concentrated dilution was detected
236 was selected as the number of cycles to be applied in the first amplification reaction of the
237 nested PCR. Optimal primers for the first round were determined by comparing the
238 efficiency of *P. chlamydospora* specific primers Pch1 and Pch2 combined with universal
239 primers ITS4 and ITS1F (Gardes and Bruns 1996; White et al. 1990), respectively.
240 According to the results obtained, the reaction was performed using universal primer ITS1F
241 and Pch2 in the first round, and Pch1 and Pch2 in the second round.
242 The first round was carried out as described earlier. The second round (final volume
243 25 µl) was carried out on a Rotor-Gene Q 5plex HRM instrument (Qiagen), and the reaction
244 mixture consisted of 12.5 µl of TB Green™ Premix Ex Taq™ (2x) (Tli RNaseH Plus;
245 Takara Bio Inc.), 0.4 µM of each primer, and 2 µl of the template DNA obtained in the first
246 round. The reaction conditions were initial denaturation at 95 ºC for 1 min, followed by 20
247 cycles (for PCR) or 40 cycles (for qPCR) of 95 °C for 5 s, 55 ºC (for PCR) or 62 ºC (for
248 qPCR) for 30 s, and 72ºC for 40 s. Melt peaks were examined to confirm amplification of
249 the correct product. Reactions included the following controls and standards: i) negative
250 controls with no DNA template in both nested PCR rounds, ii) the product of the negative
251 control for the first round in the second round, and iii) Pch gBlock standard solutions
252 (5×10^8 and 5×10^5 copies per reaction). Each laboratory sample was run in four replicates,

and fields samples were run in duplicate. Positive products of qPCR obtained from the first field samples analyzed were confirmed by 1.5% agarose gel electrophoresis and were visualized under UV light. Confirmed positive products were sequenced by Macrogen sequencing service (Macrogen Europe, Amsterdam, The Netherlands).

To determine the number of copies amplified by each reaction, the previously developed standard curves were imported using the Rotor-Gene Q software. One of the Pch gBlock standard solutions included in each qPCR was used to calibrate the imported standard curve. The mean Cq values for each unknown sample were used to calculate the number of copies per reaction.

Linear regression analysis was performed on the number of *P. chlamydospora* conidia counted by microscopy vs. the corresponding Cq values and DNA copy number using the function *lm* of the 'stats' package of R v. 3.6.0 (R Core Team 2019).

Dispersal patterns of *P. chlamydospora*. To study the temporal dispersal patterns of *P. chlamydospora*, the proportion of the total seasonal DNA (PSDNA) was calculated for each vineyard and year as the proportion of *P. chlamydospora* DNA found in traps on a particular date (the number of copies per reaction) over the total DNA found over the entire season. PSDNA values were then regressed over time, which was expressed as: (i) day of the season (DOS, starting on 1 November, when all vine leaves had fallen); (ii) thermal time (TT); or (iii) hydro-termal time (HTT). TT and HTT are both forms to express the time in physiological units (Lovell et al. 2004), and consists on sums of daily rates from a function that account the effect of temperature (in the case of TT) or temperature and moisture (in the case of HTT) on the biological process (i.e., the pycnidial development and inoculum dispersal of *P. chlamydospora*). For TT, daily values of relative mycelial growth rate (MGR) were accumulated; MGR was selected because there is no information

about the effect of temperature on pycnidial development and inoculum dispersal of *P. chlamydospora*. MGR values range from 0 to 1 and were calculated as a function of temperature, as described later in this paragraph. For HTT, daily values of MGR were also accumulated, but MGR = 1 on rainy days, i.e., on days with R > 0 mm. MGR was calculated by regressing data from Tello et al. (2009), who assessed the colony diameter of 57 isolates of *P. chlamydospora* collected in Spain every 2 days during 2 months at temperatures ranging from 5 to 35ºC (5ºC intervals), and then calculated the mean growth rate at each temperature. The effect of temperature on mycelial growth was then described by a β equation of Analytis (1977), in the form: $y = a \times Teq^b \times (1 - Teq)^c$, in which *y* is the growth rate (calculated by dividing the daily average growth at any temperature by that at the optimal temperature); *a*, *b*, and *c* are the equation parameters; and *Teq* is an equivalent of temperature calculated as *Teq = (T – Tmin)/(Tmax – Tmin)*, in which *T* is the temperature regime, and *Tmin* and *Tmax* are minimal and maximal temperatures for mycelium growth, respectively (5 and 40ºC, respectively). The *nls* function of the R 'stats' package was used to estimate the parameters, and the *epi.ccc* function of the R 'epiR' package (Stevenson 2012) was used to calculate CCC (Lin 1989). Parameter estimates were as follows: a = 30.02 ± 13.34, b = 2.70 ± 0.34, and c = 2.18 ± 0.28, with R^2 = 0.979 and concordance correlation coefficient (CCC) = 0.991.

Non-linear logistic and Gompertz equations were fit to the data by using the *nls* function in the following forms (Madden et al. 2007): $y = 1/(1 + a \times e^{-b \times t})$ for non-linear logistic equations, and $y = e^{-a \times e^{-b \times t}}$ for Gompertz equations. In these equations, *y* is the PSDNA, *a* and *b* are the equation parameters, and *t* is the time expressed as either DOS, TT, or HTT. Goodness-of-fit of the different equations was assessed by using the adjusted R^2, the magnitude of the standard error of the equation parameters, the coefficient of residual mass (CRM), and the CCC (Nash and Sutcliffe 1970; Lin 1989). The adjusted

R^2 was estimated by conducting a linear regression between the observed values (i.e., PSDNA) and the model predicted values; the linear regression was conducted with the *lm* function of the R 'stats' package.

Effect of rain on *P. chlamydospora* dispersal. The Bayes' theorem (Madden et al. 2007) was used to calculate the posterior probability of predicting the presence of *P. chlamydospora* DNA in traps based on the following rainfall cut-off values: ≥ 0.2, ≥ 1, ≥ 2, ≥ 3, ≥ 4, and ≥ 5 mm of rain. DNA presence in a trap and rain during the exposure period of the trap in the vineyard was categorized as 0 (no DNA or R < cut-off value) or 1 (DNA is present or R ≥ cut-off value). Contingency tables (2 × 2) were prepared in which cells were: 0 - 0 (no DNA and no R); 1 - 1 (DNA present and R); 0 - 1 (no DNA and R); and 1 - 0 (DNA present and no R). The true positive proportion (TPP), false negative proportion (FNP), false positive proportion (FPP), and true negative proportion (TNP) were then determined for each cut-off value. The prior probabilities of *P. chlamydospora* DNA being present in the trap, i.e., P (O+), or not, i.e., P (O-), were computed, and the posterior probability of prediction given each rainfall cut-off threshold was calculated. To study in more detail the false negative proportion (the cases in which DNA was dispersed without rain), a *t*-test was conducted to assess the effect of rain on the quantity of DNA detected; i.e., to evaluate if the quantity of DNA collected in the periods without rain was different from that collected in the periods with rain. The t-test was computed by running the *t.test* function of the R 'stats' package; this function performs a "Welch Two Sample t-test" suitable for non-normal large populations (N>30) with unequal variances (Ruxton 2006).

RESULTS

Efficiency of the DNA extraction. A significant linear relationship (P <0.001; R^2 = 0.968) was found between conidial counts in suspension C and Cq values obtained from two sets of DNA samples (Fig. 1). In one set, DNA was extracted from each of the seven 10-fold dilutions (D1-D7) of suspension C distributed on tapes. In a second set, the DNA was extracted from the most concentrated dilution (D1) placed on a tape, and the DNA extract (rather than the spore suspension) was subjected to 10-fold dilutions.

Quantitative PCR analysis. Melting analysis confirmed the amplification of the correct products, and no amplifications were observed for the negative controls. An R^2 = 0.99 and reaction efficiency of 96% were obtained based on the standard curve constructed with 10-fold dilutions of the Pch gBlocks® gene fragments ranging from 5×10^9 to 5 copies per reaction (Fig. 2). The qPCR limit of detection was 36 fg of gDNA of *P. chlamydospora* and 50 copies using the Pch gBlocks® gene fragments as standards (Tables 1 and 2). A Cq value of 31.85 which corresponded with the limit of detection was set up as threshold for the cutoff for false positive reactions (Table 2).

For conidial suspensions A and B, the number of *P. chlamydospora* conidia as determined by microscopy was significantly related to DNA copy numbers as determined by qPCR, i.e., qPCR provided a good estimate of the number of conidia detected on the tapes (R^2 = 0.729 and P = 0.019; Fig. 3). Thus, the quantity of DNA of *P. chlamydospora* found in traps was expressed as the number of conidia/cm^2 of trap.

Dynamics of *P. chlamydospora* DNA dispersal. DNA of *P. chlamydospora* was detected in all of the vineyards and years, although differences were evident in its frequency and quantity. *P. chlamydospora* DNA was detected consistently throughout the season in

Ontinyent and Logroño in 2015/2016 and 2016/2017, but was detected only three times in Logroño 2017/2018 (Fig. 4 and 5).

In Ontinyent 2015/2016, a DNA quantity corresponding to 4.7×10^5 *P. chlamydospora* conidia/cm^2 was detected over the entire sampling period; the DNA was first detected in mid-November, and a low quantity was detected until late February (Fig. 4A). In this season, only 45 mm of rain fell, and *P. chlamydospora* DNA was frequently detected in weeks without rain, mainly during December and January. In Ontinyent 2016/2017, more DNA of *P. chlamydospora* (corresponding to 2.6×10^5 conidia/cm^2) was detected than in the previous season; the DNA was also first detected in mid-November, and peaks occurred in mid-December and late January. In this season, 582 mm of rain fell and was distributed throughout the sampling period; most of the DNA was detected in weeks with rain, except in April (Fig. 4B).

In Logroño 2015/2016, a DNA quantity corresponding to 1.5×10^6 *P. chlamydospora* conidia/cm^2 was detected over the entire sampling period; most of this DNA was detected from November to the beginning of February. In this season, 300 mm of rain fell and was distributed throughout the season. DNA was not detected in March, although rain was frequent in that month, and DNA was detected only twice in April (Fig. 5A). In Logroño 2016/2017, less *P. chlamydospora* DNA (corresponding to a total of 3.4 $\times10^4$ conidia/cm^2) was detected than in the previous season; the DNA was not detected until the beginning of December, and was mainly detected during December and from February to April. In this season, 275 mm of rain fell and was distributed throughout the season; most of the DNA was detected in weeks with rain, except in April (Fig. 5B). In Logroño 2017/2018, a DNA quantity corresponding to 3.18×10^4 *P. chlamydospora* conidia/cm^2 was detected over the entire sampling period. Although 421 mm of rain fell and was distributed throughout the sampling period, the DNA was detected only three

376 times: in mid-November (in a period without rain), at the end of February, and in early
377 April (Fig 5C).
378
379 **Dispersal patterns of *P. chlamydospora.*** The pattern of DNA dispersal (expressed
380 as PSDNA) over time (expressed as DOS) was similar among locations and years, except
381 for Ontinyent 2015/2016 (Fig. 6A). In the other locations and seasons, the DNA of *P.*
382 *chlamydospora* was first detected in the second half of November, and most of the DNA
383 was detected from December to early April (DOSs 30 to 120 in Fig. 6A). The detection of
384 DNA in Ontinyent began later in 2015/2016 than in the other years and locations, and most
385 of the DNA was found from February to April (DOSs 120 to 190 in Fig. 6A). The logistic
386 and Gompertz equations relating PSDNA to DOS had $R^2 < 0.5$ and CCC< 0.7 (Fig. 6A and
387 Table 3).
388 When PSDNA was regressed against thermal time (TT), the pattern was quite
389 similar among years and locations, with the exception of Ontinyent 2015/2016. Equations
390 relating PSDNA to TT had $R^2 < 0.31$ and CCC< 0.5 (Fig. 6B and Table 3). When
391 hydrothermal time (HTT) was used as the independent variable instead of TT, the pattern
392 of PSDNA was similar for all years and locations, indicating an important role of rainfall
393 in the dispersal of *P. chlamydospora*: both logistic and Gompertz equations had $R^2 > 0.7$
394 and CCC = 0.87 (Fig. 6C,Table 3 and Supplementary figure S1).
395
396 **Effect of rain on *Phaeomoniella chlamydospora* dispersal.** Considering the whole
397 dataset (data from 146 weeks from all seasons and vineyards), the DNA of *P.*
398 *chlamydospora* was detected in 17 of 23 weeks with no rain (74.0%), and in 68 of 123
399 weeks with rain (55.3%). In 55 cases, rain was recorded and DNA of *P. chlamydospora*
400 was not (44.7%).

With a cut-off value of R ≥0.2 mm, the TPP was 0.80 and the TNP was 0.10, with an overall accuracy of 0.51 (Table 4). When higher rainfall cut-off values were considered as predictors of *P. chlamydospora* dispersal, the overall accuracy decreased, and the posterior probabilities of correct predictions were reduced (Table 4).

The posterior probabilities of correctly predicting *P. chlamydospora* dispersal (*P*(P+|O+)) and no dispersal (*P*(P-|O-)) based on R ≥0.2 mm were 0.55 and 0.78, respectively. The posterior probability of predicting a dispersal that did not occur (*P*(P+|O-)) was 0.45 (Table 4), indicating that the use of rain as a predictor of *P. chlamydospora* dispersal generated several false positives. These false positives occurred, for instance, in Rioja 2015/2016, when the repeated late-season rains (in March) did not result in *P. chlamydospora* DNA detection, probably because the inoculum was depleted by previous rains. False negatives also occurred in Rioja 2017/2018, where the quantity of DNA found during the season was very low compared to the other vineyards. Therefore, false positives seem to be related to the scarcity of *P. chlamydospora* inoculum in the vineyard.

The posterior probability of failing to predict the dispersal (*P*(P-|O+)) was 0.22, indicating that using ≥0.2 mm of rain as a predictor of *P. chlamydospora* dispersal generated some false negatives. Even though false negatives may result in the underestimation of inoculum dispersal in the vineyard and consequently an underestimation of a potential infection, the *P. chlamydospora* DNA found in traps during these false negatives accounted for only 4% of the total DNA detected during the study, indicating that although *P. chlamydospora* can disperse during periods without rain, the inoculum load in these periods may be very low compared to the total inoculum of the season. This was also confirmed by the comparison of the distributions of the conidia trapped in weeks with and without rain (Fig. 7; $P < 0.001$).

DISCUSSION

In the current study, we investigated the temporal dispersal patterns of *P. chlamydospora* in two viticultural areas of eastern (Ontinyent) and northern (Logroño) Spain, during two and three growing seasons, respectively. In these areas and in other areas of Spain, *P. chlamydospora* has been previously isolated from plants in vineyards (Armengol et al. 2001; Gramaje et al. 2009; Tello et al. 2010) and nurseries (Gramaje et al. 2009; Aroca et al. 2010). We consistently detected the DNA of *P. chlamydospora* in spore traps exposed from November to April in both locations and in all seasons, except in Logroño in 2017/2018, where the pathogen was detected only three times.

The inoculum of *P. chlamydospora* detected during the season differed substantially among vineyards and years; these differences were probably due to differences in the quantity of primary inoculum, which in turn can be affected by multiple epidemiological and agronomical factors, including the incidence of GTDs in the vineyard. In this work, we selected commercial vineyards in which vines showed symptoms of esca. However, the incidence of the disease could vary from vineyard to vineyard and from year to year. Differences in the abundance *P. chlamydospora* conidia were especially evident between Logroño 2015/2016 (150×10^4 conidia/cm^2 of trap) and Logroño 2016/2017 (3.18×10^4 conidia/cm^2 of trap). Those vineyards were less than 500 m apart, suggesting that the inoculum is mainly dispersed short distances, probably by splashes of raindrops (Aylor 2017).

Despite these differences in the quantities of *P. chlamydospora* DNA found in traps, the dispersal patterns throughout the growing seasons were similar among vineyards and years: the DNA was first detected in the second half of November, and most of the DNA was detected from December to the beginning of April. This pattern of *P. chlamydospora*

451 detection generally agrees with previous reports (Eskalen and Gubler 2001; Larignon and
452 Dubos 2000; Quaglia et al. 2009), but differs in some ways. For example, Quaglia et al.
453 (2009) did not trap conidia from January to March, and Larignon and Dubos (2000) did not
454 trap conidia from February to June. Comparison between these and our findings is difficult,
455 because different methodologies were used to detect and quantify the inoculum of *P.*
456 *chlamydospora*. As in the current research, the two previous studies exposed microscope
457 slides in the vineyards and replaced them weekly. In contrast to the current research,
458 however, the two previous studies then removed the spores with water and plated the
459 suspension on different culture media. Because qPCR is probably more sensitive than
460 plating on culture media, that *P. chlamydospora* was detected over wider periods in the
461 current study than in the two earlier studies is not surprising.

462 For all years and locations, the dynamics of *P. chlamydospora* dispersal were best
463 explained when time was expressed as hydro-thermal time. Hydro-thermal time is a
464 physiological time that accounts for the effects of both temperature and rain, and that has
465 been previously used to describe the development of different pathogens, including
466 Botryosphaeriaceae species affecting grapevines (Silva et al. 2018; Onesti et al. 2018). In
467 the equations developed in the current study, moisture was accounted for by rain events. It
468 is plausible that rain can contribute to (i) the development of pycnidia and masses of
469 conidia, and to (ii) the splash-dispersal of conidia from pycnidia. For (i), the rain events
470 were likely associated with periods of high RH that in other pycnidia-producing fungi
471 promote, together with moderate temperatures, the production of pycnidia and the
472 extrusion of the conidia (Anco et al. 2013; Lalancette et al. 2003; Onesti et al. 2017). In the
473 case of *P. chlamydospora*, no information is available about the effect of weather on the
474 production of pycnidia; in the current study, we inferred the effect of temperature from a
475 previous experiment regarding mycelial growth (Tello et al. 2010). Specific studies are

476 needed to verify whether the temperature relationships for colony growth and the
477 development of pycnidia are similar. Moreover, because environmental conditions may
478 also affect the dispersal of other pathogens associated with Petri disease and esca, studies
479 should be also conducted to determine how the dispersal of these other pathogens is related
480 to environmental conditions.

481 When rain was evaluated as a predictor of *P. chlamydospora* dispersal, high
482 proportions of false negatives (FNP) and false positives (FPP) were observed. FNP was
483 related to cases in which rain was not recorded but *P. chlamydospora* DNA was detected
484 in traps; such dispersal involved only the 4% of the total DNA detected throughout the
485 seasons. Aerial dissemination of *P. chlamydospora* in periods with no rain may involve
486 conidia produced by conidiophores extending from hyphae (i.e., not produced in pycnidia)
487 or fragments of cirri that extruded from pycnidia in previous moist periods and that have
488 not been dispersed by rain splashes; as these cirri desiccate and crumble, perhaps their
489 fragments can become airborne. Aerial dissemination of pycnidiospores in periods with no
490 rain has been previously reported for other pathogens that produce pycnidia (Shulhani et
491 al. 2018).

492 An important outcome of this study was the development and testing of a PCR-
493 based method for the detection and quantification of *P. chlamydospora* in spore traps; to
494 our knowledge, no similar methods have been published. Previous studies on conidial
495 dispersal patterns of *P. chlamydospora* relied on the microscopic counting of spores or on
496 the counting of colony forming units on culture media (Eskalen and Gubler 2001; Larignon
497 and Dubos 2000; Quaglia et al. 2009; van Niekerk et al. 2010). These techniques are time-
498 consuming and less specific and sensitive than molecular methods for detecting and
499 quantifying fungal pathogens in the environment (Billones-Baaijens et al. 2018).

In a preliminary experiment in the current study, a previously developed Taqman assays targeting the ITS region (Martín et al. 2012) was tested using gDNA from *P. chlamydospora*, and we found that the sensitivity of detection was low (*data not shown*). However, we still considered the ITS region to be preferred target for molecular detection of *P. chlamydospora*. The choice of the locus used for qPCR assays largely depends on the aim of the study. Although multicopy genes allow the detection of lower DNA amounts, single-copy genes give more precise measurements of DNA copy number (Longo et al. 2013; Tellenbach et al. 2010). In the qPCR method developed in the current study, we selected the ITS because we expected that the quantity of DNA of *P. chlamydospora* to be low in the spore traps located in the vineyards. For the same reason, we increased the sensitivity of the qPCR by using a nested approach; in this approach, almost the entire locus was initially amplified by conventional PCR, and the resulting product was then quantified with the specific primer combination in a second step. In a previous study, a nested-PCR using primers ITS4-ITS6 and Pch1-Pch2 was optimized for detecting *P. chlamydospora* in DNA extracted from soil, water, callusing medium, and grapevine wood (Retief et al. 2006). With the synthetic single copy of the target fragment (gBlocks®, IDT Technologies) as standards, the qPCR limit of detection obtained in our study was 36 fg of gDNA of *P. chlamydospora* and 50 copies of the target fragment.

In the current study, we used glass microscope slides for the weekly monitoring of the airborne propagules of *P. chlamydospora* in the vineyards and ceramic beads to remove them from the tapes and for tissue lysis according to a protocol described by Billones-Baaijens et al. (2018) with minor modifications. In a preliminary test using non-exposed and field-exposed tapes that were artificially infested with *P. chlamydospora* conidia in the laboratory, the commercial kit selected for DNA extraction was found to be efficient and to provide consistent results. The significant linear relationship between conidial counts in

suspension C and Cq values obtained from DNA samples (Fig. 1) confirmed the efficiency of the DNA extraction protocol. The linear relationship between *P. chlamydospora* conidia counts and DNA copy numbers (Fig. 3) enabled us to estimate the number of conidia detected on the tapes.

The equations developed here to describe the dynamics of *P. chlamydospora* dispersal could be used to predict periods of high risk of dispersal of the pathogen; before they are used however, the equations should be validated with independent data collected in different years, locations, and viticultural systems (Rossi et al. 2010). Identifying the periods of high risk of dispersal may contribute to the practical management of this pathogen. During high risk periods, for instance, pruning should be avoided and pruning wounds should be protected (Berbegal et al. 2019; Gramaje et al. 2018; Mondello et al. 2018). Previous reports have been inconsistent about the best period for pruning in order to reduce the risk of *P. chlamydospora* infection. In South Africa, van Nieker et al. (2011) indicated that late-winter wounds were more susceptible to infection than early season wounds. In contrast, Larignon and Dubos (2000) in France observed that, with early pruning (December, January), the pathogen was able to infect during a longer period and that infections were more serious than with later pruning. In Italy, Serra et al. (2008) found infections caused by *P. chlamydospora* for up to 4 months after pruning. In California, Eskalen et al. (2007) showed that wounds were susceptible to *P. chlamydospora* throughout the summer, and in Spain, Elena and Luque (2016) did not detect seasonal differences in wound susceptibility to *P. chlamydospora* when fall and winter pruning were compared. Results of our work indicate that the period of highest risk for *P. chlamydospora* may vary from year to year or among locations depending on weather conditions.

The present research increases our understanding of the epidemiology of the main causal agent of Petri disease and esca, *P. chlamydospora.* Once the equation developed

here is validated, it should be incorporated into a decision support system that will help growers adopt effective practices for controlling GTDs (Rossi et al. 2010).

ACKNOWLEDGMENTS

Financial support for carrying out this research was provided by transnational funding Bodies, being partners of the H2020 ERA-net project, CORE Organic Cofund, and the cofund from the European Commission (PCI2018-093015 / Project BIOVINE). Part of the research was funded by CAR (Government of La Rioja, Spain), project number R-03-16. We thank the "Cooperativa Vinícola Onteniense" for providing the vineyards in Ontinyent. We thank S. Arizmendi, S. Catalá, V. Morant and P. Yécora for the technical support. C. Berlanas was supported by the FPI-INIA program from the INIA. D. Gramaje was supported by the Ramón y Cajal program, Spanish Government (RYC-2017-23098). Financial support by the Viticulture Research Network "RedVitis" (AGL2015-70931-REDT) for C. Berlanas during her 1 month stay at UPV is gratefully acknowledged.

LITERATURE CITED

Agustí-Brisach, C., León, M., García-Jiménez, J., and Armengol, J. 2015. Detection of grapevine fungal trunk pathogens on pruning shears and evaluation of their potential for spread of infection. Plant Dis. 99: 976-981.

Analytis, S. 1977. On the relation between biological development and temperature of some plant pathogenic fungi. Phytopathol. Z. 90:64-76.

Anco, D. J., Madden, L. V., and Ellis, M. A. 2013. Effects of temperature and wetness duration on the sporulation rate of *Phomopsis viticola* on infected grape canes. Plant Dis. 97: 579-589.

576 Armengol J., Vicent A., Torné L., García-Figueres F. and García-Jiménez J., 2001. Fungi
577 associated with esca and grapevine declines in Spain: a three-year survey. Phytopathol.
578 Mediter. 40: S325-S329.
579 Aroca, A., Gramaje, D., Armengol, J., García-Jiménez, J., and Raposo, R. 2010. Evaluation
580 of grapevine nursery process as a source of *Phaeoacremonium* spp. and *Phaeomoniella*
581 *chlamydospora* and occurrence of trunk disease pathogens in rootstock mother vines in
582 Spain. Eur. J. Plant Pathol. 126: 165-174.
583 Aylor, D. 2017. Aerial dispersal of pollen and spores. APS Press, St Paul, MN.
584 Baloyi, M. A., Hallen, F., Mostert, L., and Eskalen, A. 2016. First report of *Phaeomoniella*
585 *chlamydospora* pycnidia as Petri disease inoculum sources in South African vineyards.
586 Plant Dis. 100: 2528.
587 Billones-Baaijens, R., Úrbez-Torres, J. R., Liu, M., Ayres, M., Sosnowski, M. R., and
588 Savocchia, S. 2018. Molecular methods to detect and quantify Botryosphaeriaceae
589 inocula causing grapevine dieback in Australia. Plant Dis. 102: 1489-1499
590 Berbegal, M., Ramón-Albalat, A., León, M. and Armengol, J. 2019. Evaluation of
591 long-term protection from nursery to vineyard provided by *Trichoderma atroviride*
592 SC1 against fungal grapevine trunk pathogens. Pest. Manag. Sci.
593 DOI:10.1002/ps.5605.
594 Bertelli, E., Mugnai, L., and Surico, G., 1998. Presence of *Phaeoacremonium*
595 *chlamydosporum* in apparently rooted grapevine cuttings. Phytopathol. Mediterr. 37:
596 79-82.
597 Bertsch, C., Ramírez-Suero, M., Magnin-Robert M., Larignon, P., Chong, J., Abou-
598 Mansour, E., Spagnolo, A., Clément, C., and Fontaine, F. 2013. Grapevine trunk
599 diseases: complex and still poorly understood. Plant Pathol. 62: 243-265.

600 Bustin, S.A., Benes, V., Garson, J.A., Hellemans, J., Huggett, J., Kubista, M., Mueller, R.,
601 Nolan, T., Pfaffl, M. W., Shipley, G.L., Vandesompele, J., and Wittwer, C. T. 2009.
602 The MIQE guidelines: minimum information for publication of quantitative real-time
603 PCR experiments. Clin. Chem. 55: 611-622.
604 Chen K.H, Miadlikowska J., Molnár K., Arnold E., U'Ren J.M., Gaya E., Gueidan C.,
605 Lutzoni F. 2015. Phylogenetic analyses of Eurotiomycetous endophytes reveal their
606 close affinities to Chaetothyriales, Eurotiales, and a new order – Phaeomoniellales.
607 Mol. Phylogenet. Evol. 85: 117-130.
608 Cloete, M., Fischer, M., Mostert, L., and Halleen, F. 2015. Hymenochaetales associated
609 with esca-related wood rots on grapevine with a special emphasis on the status of esca
610 in South African vineyards. Phytopathol. Mediterr. 54: 299-312.
611 Crous, P. W., and Gams, W. 2000. *Phaeomoniella chlamydospora* gen. et comb. nov., a
612 causal organism of Petri grapevine decline and esca. Phytopathol. Mediterr. 39: 112-
613 118.
614 Edwards, J., and Pascoe, I. G. 2001. Pycnidial state of *Phaeomoniella chlamydospora*
615 found on 'Pinot Noir' grapevines in the field. Australasian Plant Pathol. 30: 67.
616 Edwards, J., Constable, F.,Wiechel, T., and Salib, S. 2007. Comparison of the molecular
617 tests – single PCR, nested PCR and quantitative PCR (SYBR_Green and TaqMan_) –
618 for detection of *Phaeomoniella chlamydospora* during grapevine nursery propagation.
619 Phytopathol. Mediterr. 46: 58-72.
620 Edwards, J., Laukart, N., and Pascoe, I. 2001. *In situ* sporulation of *Phaeomoniella*
621 *chlamydospora* in the vineyard. Phytopathol. Mediterr. 40: 61-66.
622 Elena, G., and Luque, J. 2016. Seasonal susceptibility of grapevine pruning wounds and
623 cane colonization in Catalonia, Spain following artificial infection with *Diplodia*
624 *seriata* and *Phaeomoniella chlamydospora*. Plant Dis. 100: 1651-1659.

625 Eskalen, A., and Gubler, W. D. 2001. Association of spores of *Phaeomoniella*
626 *chlamydospora*, *Phaeoacremonium inflatipes*, and *Pm. aleophilum* with grapevine
627 cordons in California. Phytopathol. Mediterr. 40S: 29-32.
628 Eskalen, A, Feliciano, J., and Gubler, W. D. 2007. Susceptibility of grapevine pruning
629 wounds and symptom development in response to infection by *Phaeoacremonium*
630 *aleophilum* and *Phaeomoniella chlamydospora*. Plant Dis. 91: 1100-1104.
631 Fischer, M., and González-García, V., 2015. An annotated checklist of European
632 basidiomycetes related to white rot of grapevine (*Vitis vinifera*). Phytopathol. Mediterr.
633 54: 281-298.
634 Fourie, P.H., and Halleen, F. 2002. Investigation on the occurrence of *Phaeomoniella*
635 *chlamydospora* in canes rootstock mother vines. Australas. Plant Path. 31: 425–427.
636 Gardes, M., and Bruns, T. 1993. ITS primers with enhanced specificity for basidiomycetes
637 - application to the identification of mycorrhizae and rusts. Mol. Ecol. 2: 113-118.
638 Giménez-Jaime, A., Aroca, A., Raposo, R., García-Jiménez, J., and Armengol, J. 2006.
639 Occurrence of fungal pathogens associated with grapevine nurseries and the decline of
640 young vines in Spain. J. Phytopathol. 154: 598–602.
641 Gramaje, D., Muñoz, R. M., Lerma, M. L., García-Jiménez, J., and Armengol, J. 2009.
642 Fungal grapevine trunk pathogens associated with Syrah decline in Spain.
643 Phytopathol. Mediterr. 48: 396-402.
644 Gramaje, D., Mostert, L., and Armengol, J. 2011. Characterization of *Cadophora luteo-*
645 *olivacea* and *C. melinii* isolates obtained from grapevines and environmental samples
646 from grapevine nurseries in Spain. Phytopathol. Mediterr. 50: S112-S126.
647 Gramaje, D., Mostert, L., Groenewald, J. Z., and Crous P. W. 2015. *Phaeoacremonium*:
648 from esca disease to phaeohyphomycosis. Fungal Biol. 119: 759-783.

649 Gramaje, D., Úrbez-Torres, J. R., and Sosnowski, M. R. 2018. Managing grapevine trunk
650 diseases with respect to etiology and epidemiology: current strategies and future
651 prospects. Plant Dis. 102: 12-39.
652 Gubler, W. D., Mugnai, L., and Surico, G. 2015. Esca, Petri and Grapevine leaf stripe
653 disease. Pages 52-56 in: Compendium of Grape Disease, Disorders, and Pets, 2nd Ed.
654 W. F. Wilcox, W. D. Gubler, and J. K. Uyemoto, eds. APS Press, St Paul, MN.
655 Halleen, F., Crous, P. W., and Petrini, O. 2003. Fungi associated with healthy grapevine
656 cuttings in nurseries, with special reference to pathogens involved in the decline of
657 young vines. Australas. Plant Path. 32: 47-52.
658 Lalancette, N., Foster, K. A., and Robison, D. M. 2003. Quantitative models for describing
659 temperature and moisture effects on sporulation of *Phomopsis amygdali* on peach.
660 Phytopathology 93:1165-1172.
661 Larignon, P., and Dubos, B. 2000. Preliminary studies on the biology of
662 *Phaeoacremonium*. Phytopathol. Mediterr. 39: 184-189.
663 Lin, L. 1989. A concordance correlation coefficient to evaluate reproducibility. Biometrics
664 45: 255–268.
665 Longo, A. V., Rodriguez, D., Da Silva, L. D., Felipe Toledo, L., Mendoza Almeralla, C.,
666 Burrowes, P. A., and Zamudio, K. L. 2013. ITS1 copy number varies among
667 *Batrachochytrium dendrobatidis* strains: implications for qPCR estimates of infection
668 intensity from field-collected amphibian skin swabs. PLOS ONE 8: e59499.
669 Madden, L. V., Hughes, G. and Van den Bosch, F. 2007. The study of plant disease
670 epidemics, eds. APS Press, St Paul, MN.

671 Martín, M.T., Cobos, R., Martín, L. and López-Enríquez, L. 2012. Real-time PCR detection
672 of *Phaeomoniella chlamydospora* and *Phaeoacremonium aleophilum*. App. Environ.
673 Microbiol. 78: 3985–3991.

674 Mondello, V., Songy, A.., Battiston, E., Pinto, C., Coppin, C., Trotel-Aziz, P. and Fontaine
675 F. 2018. Grapevine trunk diseases: a review of fifteen years of trials for their control
676 with chemicals and biocontrol agents. Plant Dis. 7: 1189-1217.

677 Moyo, P., Allsopp, E., Roets, F., Mostert, L., and Halleen, F. 2014. Arthropods vector
678 grapevine trunk disease pathogens. Phytopathology 104: 1063-1069.

679 Nash, J. and Sutcliffe, J. 1970. River flow forecasting through conceptual models part I. J.
680 Hydrol. 10: 282-290.

681 Onesti, G., González-Domínguez, E., and Rossi, V. 2017. Production of pycnidia and
682 conidia by *Guignardia bidwellii*, the causal agent of grape black rot, as affected by
683 temperature and humidity. Phytopathology 107: 173-183.

684 Onesti, G., González-Domínguez, E., Manstretta, V., Rossi, V., 2018. Release of
685 *Guignardia bidwellii* ascospores and conidia from overwintered grape berry
686 mummies in the vineyard. Aust. J. Grape Wine Res. 24: 136–144.

687 Overton, B. E., Stewart, E. L., Qu, X., Wenner, N. G., and Christ, B. J. 2004. Qualitative
688 real-time PCR SYBR® Green detection of Petri disease fungi. Phytopathol. Mediterr.
689 43: 403-410.

690 Pouzoulet, J., Mailhac, N., Couderc, C., Besson, X., Dayde, J., Lummerzheim, M., and
691 Jacques A. 2013. A method to detect and quantify *Phaeomoniella chlamydospora* and

692 *Phaeoacremonium aleophilum* DNA in grapevine-wood samples. Appl. Microbiol.
693 Biot. 97: 10163-10175.
694 Quaglia, M., Covarelli, L., and Zazzerini, A. 2009. Epidemiological survey on esca disease
695 in Umbria, central Italy. Phytopathol. Mediterr. 48: 84-91.
696 R Core Team. 2019. R: A language and environment for statistical computing. R
697 Foundation for Statistical Computing, Vienna, Austria. URL (https://www.R-
698 project.org/).
699 Ridgway, H. J., Sleight, B. E., and Stewart, A. 2002. Molecular evidence for the presence
700 of *Phaeomoniella chlamydospora* in New Zealand nurseries, and its detection in
701 rootstock mothervines using species-specific PCR. Australas. Plant Path. 31: 267-271.
702 Retief, E., McLeod, A., and Fourie, P. H. 2006. Potential inoculum sources of
703 *Phaeomoniella chlamydospora* in South African grapevine nurseries. Eur. J. Plant
704 Pathol. 115: 331-339.
705 Rolshauen, P. E., Úrbez-Torres, J. R., Rooney-Latham, S., Eskalen, A., Smith, R. J., and
706 Gubler, W. D. 2010. Evaluation of pruning wound susceptibility and protection against
707 fungi associated with grapevine trunk diseases. Am. J. Enol. Viticult. 61: 113-119.
708 Rossi V, Giosuè S, Caffi T. 2010. Modelling plant diseases for decision making in crop
709 protection. In: Oerke E-C, Gerhards R, Menz G, Sikora RA, editors. Precision Crop
710 Protection—the Challenge and Use of Heterogeneity. Dordrecht: Springer Netherlands.
711 pp. 241-258.
712 Ruxton, G. D. 2006. The unequal variance t-test is an underused alternative to Student's t-
713 test and the Mann–Whitney U test. Behav. Ecol. 17: 688–690.
714 Serra, S., Mannoni, M.A., and Ligios, V. 2008. Studies on the susceptibility of pruning
715 wounds to infection by fungi involved in grapevine wood diseases in Italy. Phytopathol.
716 Mediterr. 47: 234-246.

717 Shulhani, R., and Shtienberg, D. 2018. Aerial dissemination of *Lasiodiplodia theobromae*
718 and *L. pseudotheobromae* pycnidiospores. In: Stensvand, A., editor. The 12th
719 International Epidemiology Workshop (IEW12). Lillehammer, Norway, 10 - 14 June.
720 Silva, F., Santos, K., Rego, T., Armengol, J., Rossi, V., Michereff, S., González-
721 Domínguez, E., 2018. Temporal conidial dispersal pattern of Botryosphaeriaceae
722 species in table-grape vineyards in Northeastern Brazil. Phytopathol. Mediterr. 57: 547–
723 556.
724 Tellenbach, C., Grünig, C. R., and Sieber, T. N. 2010. Suitability of quantitative real-time
725 PCR to estimate the biomass of fungal root endophytes. Appl. Environ. Microbiol. 76:
726 5764-5772.
727 Tello, M. L., Gramaje, D., Gómez, A., Abad-Campos, P., Armengol, J., 2010. Analysis of
728 phenotypic and molecular diversity of *Phaeomoniella chlamydospora* isolates in Spain.
729 J. Plant Pathol. 92: 195-203.
730 van Niekerk, J. M., Calitz, J., Halleen, F., and Fourie, P. 2010. Temporal spore dispersal
731 patterns of grapevine trunk pathogens in South Africa. Eur. J. Plant Pathol. 127: 375-
732 390.
733 van Niekerk, J. M., Halleen, F., and Fourie, P. 2011. Temporal susceptibility of grapevine
734 pruning wounds to trunk pathogen infection in South African grapevines. Phytopathol.
735 Mediterr. 50: S139-S150.
736 White, T. J., Burns, T., Lee, S., and Taylor, J. 1990. Amplification and direct sequencing
737 of fungal ribosomal RNA genes for phylogenetics. In: Innis, M. A., Gelfand, D. H.,
738 Sninsky, J. J. et al., eds. PCR Protocols: a Guide to Methods and Applications.
739 Academic Press, San Diego, California. pp. 315-322.

Whiteman, S. A, Stewart, A., Ridgway, H. J., and Jaspers, M. V. 2007. Infection of rootstock mother-vines by *Phaeomoniella chlamydospora* results in infected young grapevines. Australas. Plant Path. 36: 198-203.

Table 1. The limit of detection of the qPCR analysis using 10-fold dilutions of the genomic DNA of *Phaeomoniella chlamydospora* (isolate Pch184).

fg of DNA/reaction	Quantification cycle (Cq)[a]	Signal ratio[b]
360,000	1.03 ± 0.01	8/8
36,000	3.20 ± 0.01	8/8
3,600	6.31 ± 0.11	8/8
360	9.18 ± 0.09	8/8
36	12.43 ± 0.09	8/8
3.6	Not detected	0/8

[a] Quantification cycle (Cq value) at which fluorescence was detected in the qPCR analysis. The Cq values are the means ± SE of two independent assays, each with four technical replicates.

[b] Number of positive samples detected out of the total number of reactions performed.

766 **Table 2**. The limit of detection of the qPCR analysis using 10-fold
767 dilutions of the Pch gBlocks® gene fragments ranging from 5×10^9 to 5
768 copies per reaction.

Copies per reaction	Quantification cycle (Cq)[a]	Signal ratio[b]
5,000,000,000	4.61 ± 0.07	8/8
500,000,000	7.78 ± 0.06	8/8
50,000,000	11.22 ± 0.07	8/8
5,000,000	14.53 ± 0.09	8/8
500,000	17.92 ± 0.05	8/8
50,000	21.43 ± 0.06	8/8
5,000	24.77 ± 0.10	8/8
500	28.42 ± 0.10	8/8
50	31.85 ± 0.13	8/8
5	Not detected	0/8

769 [a] Quantification cycle (Cq value) at which fluorescence was detected in the qPCR
770 analysis. The Cq values are the means ± SE of two independent assays, each with four
771 technical replicates.
772 [b] Number of positive samples detected out of the total number of reactions performed.
773
774

775

776 **Table 3.** Parameters and goodness-of-fit indexes of the equations used to describe the effect of
777 different physiological units on the proportion of the total seasonal inoculum (PSDNA) of
778 *Phaeomoniella chlamydospora* detected in three vineyards located in Ontinyent and Logroño, Spain,
779 from 2016 to 2018.

Physiological units[a]	Equation[b]	Estimated parameters[b]		Goodness of fit[c]		
		a	***b***	***R²***	**CRM**	**CCC**
DOS	Logistic	6.676 (2.486)	0.025 (0.004)	0.494	-0.006	0.670
	Gompertz	2.537 (0.576)	0.018 (0.003)	0.493	0.006	0.669
TT	Logistic	3.409 (1.200)	0.089 (0.020)	0.289	-0.041	0.482
	Gompertz	1.738 (0.389)	0.068 (0.015)	0.305	0.006	0.499
HTT	Logistic	12.443 (3.915)	0.072 (0.008)	0.771	0.007	0.873
	Gompertz	3.871 (0.765)	0.051 (0.006)	0.765	0.028	0.870

780 [a] DOS: days of the season starting on 1 November. TT: thermal time; daily values of temperature were accumulated
781 as a function of mycelial growth rate (MGR) as described in the Materials and Methods. HTT: hydrothermal time; like
782 TT but the days with rain take a value of 1, regardless the values of MGR.

783 [b] Regression equations were $y = 1/(1+a\times\exp(-b\times t))$ for logistic, and $y = \exp(-a\times\exp(-b\times t))$ for Gompertz, in which y is
784 PSDNA, a and b are the equation parameters, and t is the time expressed by the different physiological units. Standard
785 errors of the estimated parameters are in parentheses.

786 [c] R^2, coefficient of determination; CRM, coefficient of residual mass; CCC, concordance correlation coefficient.

787

788

789

790 **Table 4.** Evaluation of rainfall for predicting the detection of *Phaeomoniella chlamydospora* DNA on
791 spore traps placed in three vineyards located in Ontinyent and Logroño, Spain, from 2016 to 2018.

Rain[a]	Proportions[b]				Overall accuracy[c]	Posterior probabilities[d]			
	TPP	FNP	FPP	TNP		(P+|O+)	(P-|O-)	(P+|O-)	(P-|O+)
≥ 0.2	0.80	0.20	0.90	0.10	0.51	0.55	0.78	0.45	0.22
≥ 1	0.55	0.45	0.69	0.31	0.45	0.53	0.62	0.47	0.38
≥ 2	0.45	0.55	0.59	0.41	0.43	0.51	0.56	0.49	0.43
≥ 3	0.40	0.60	0.56	0.44	0.42	0.50	0.54	0.50	0.45
≥ 4	0.35	0.65	0.56	0.44	0.39	0.47	0.53	0.53	0.47
≥ 5	0.28	0.72	0.51	0.49	0.37	0.44	0.50	0.56	0.50

792 [a] Total quantities of rainfall (mm) that were used as cut-off values to define a rain event.

793 [b] TPP (true positive proportion, or sensitivity): periods when rain = 1 and DNA detection = 1 divided by the total number
794 of periods with detection. TNP (true negative proportion, or specificity): periods when rain = 0 and DNA detection = 0
795 divided by the total number of periods with no detection. FPP (false positive proportion): periods when rain = 1 and DNA
796 detection = 0 divided by the total number of periods with no detection. FNP (false negative proportion): periods when rain
797 = 0 and DNA detection = 1 divided by the total number of periods with detection.

798 [c] Overall accuracy calculated as the proportion of correct predictions.

799 [d] P(P+|O+): posterior probability that *P. chlamydospora* DNA was detected when predicted based on rainfall amount. P(P-
800 |O-): posterior probability that DNA was not detected when not predicted. P(P+|O-): posterior probability that DNA was
801 not detected when predicted. P(P-|O+): posterior probability that DNA was detected when not predicted.

802

Figure captions

Fig. 1. Relationship between number of *Phaeomoniella chlamydospora* conidia in conidial suspension series C and quantification cycle (Cq) values obtained from two sets of DNA samples. In one set, the spore suspension was diluted (seven 10-fold dilutions, dilution D1–D7) and placed on tapes before DNA was extracted (dots). In a second set, DNA was extracted from dilution D1 and the extracted DNA was then subjected to 10-fold dilutions (triangles). Values are means ± SE of four replicates. The grey dashed line represents the linear regression model fit to the data ($y = -3.644x + 27.903$) with $R^2 = 0.968$ and $P < 0.001$.

Fig. 2. Standard curve for *Phaeomoniella chlamydospora* inoculum quantification. The curve was constructed using 10-fold dilutions of the Pch gBlocks® gene fragments containing from 5×10^9 to 5 copies per reaction. Values are means of four replicates. The reaction efficiency was 96%. The grey dashed line represents the linear regression of the standard curve ($y = -3.409x + 37.479$) with $R^2 = 0.999$ and $P < 0.001$.

Fig. 3. Relationship between conidia counts obtained using light microscopy from conidial suspension series A and B and DNA copy number of *Phaeomoniella chlamydospora*. Conidia were counted in suspensions using a haemocytometer and a microscope. The suspensions were then added to tapes before DNA was extracted and subjected to qPCR for determination of DNA copy number. Values are means ± SE of four replicates. The grey dashed line represents the linear regression model fit to the data ($y = 0.808x + 2.679$) with $R^2 = 0.729$ and $P = 0.019$.

Fig. 4. *Phaeomoniella chlamydospora* inoculum detected on microscope slide traps in two vineyards in Ontinyent, Spain, in seasons 2015/2016 (A) and 2016/2017 (B). Black dots indicate the inoculum expressed as the average number of conidia/cm^2 on five traps replaced weekly. The black line and grey bars represent the daily average temperature and the daily accumulated rain, respectively.

828 **Fig. 5.** *Phaeomoniella chlamydospora* inoculum detected in microscope slide traps in two
829 vineyards in Logroño, Spain, in seasons 2015/2016 (A), 2016/2017 (B), and 2017/2018
830 (C). Black dots indicate the inoculum expressed as the average number of conidia/cm^2 on
831 five traps replaced weekly. The black line and grey bars represent the daily average
832 temperature and the daily accumulated rain, respectively.
833 **Fig. 6.** Proportion of the total seasonal inoculum (PSDNA) of *Phaeomoniella*
834 *chlamydospora* detected over time on microscope slide traps in vineyards in 2015/2016
835 (dots), 2016/2017 (triangles), and 2017/2018 (squares): black and grey symbols indicate
836 vineyards located in Ontinyent and Logroño, respectively. Time is expressed as day of the
837 year starting on 1 November (DOS, A), thermal time (TT, B) or hydro-thermal time (HTT,
838 C). Logistic (solid line) and Gompertz (dotted line) equations were fit to the data (Table
839 3).
840 **Fig. 7.** Boxplots of the distributions of the DNA of *Phaeomoniella chlamydospora* detected
841 on microscope slide traps in weeks without rain (n=72) or with rain (n=74). qPCR was used
842 to detect and quantify the inoculum, which is expressed as the average number of
843 conidia/cm^2 on five traps replaced weekly. Boxes include the 2nd and 3rd quartiles; the
844 thick black line is the median; whiskers extend to minimum and maximum values; and the
845 dots are the outliers.

846

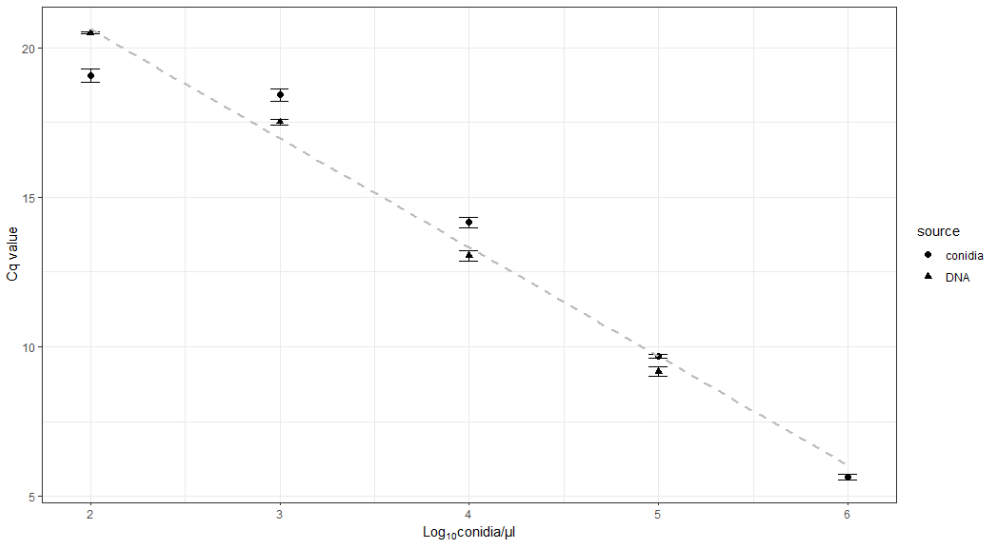

Figure captions

Fig. 1. Relationship between number of Phaeomoniella chlamydospora conidia in conidial suspension series C and quantification cycle (Cq) values obtained from two sets of DNA samples. In one set, the spore suspension was diluted (seven 10-fold dilutions, dilution D1–D7) and placed on tapes before DNA was extracted (dots). In a second set, DNA was extracted from dilution D1; the extracted DNA was then subjected to 10-fold dilutions before each dilution was distributed on tapes (triangles). Values are means + SE of four replicates. The grey dashed line represents the linear regression model fit to the data (y = -3.644x + 27.903) with R2 = 0.968 and P <0.001.

277x152mm (96 x 96 DPI)

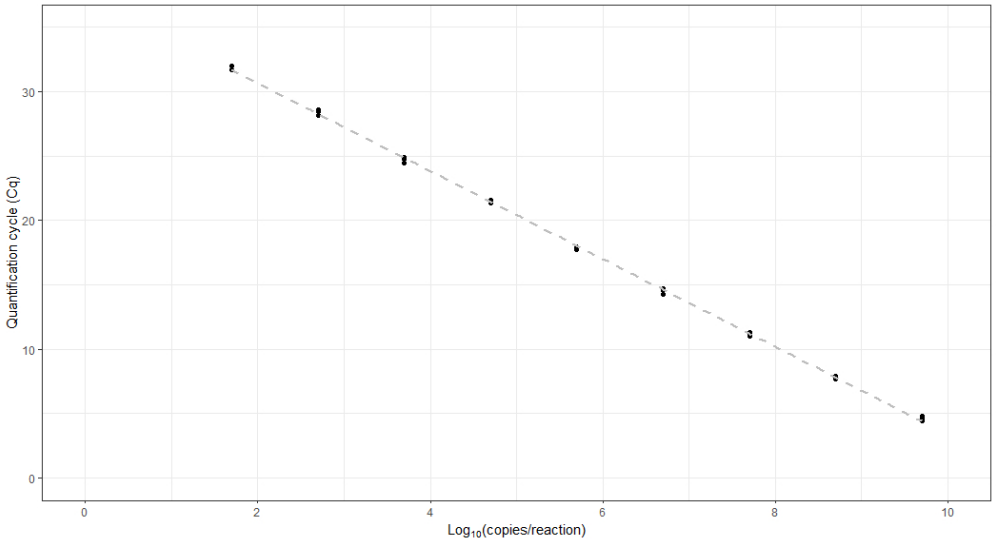

Fig. 2. Standard curve for Phaeomoniella chlamydospora inoculum quantification. The curve was constructed using 10-fold dilutions of the Pch gBlocks® gene fragments containing from 5×109 to 5 copies per reaction. Values are means of four replicates. The reaction efficiency was 96%. The grey dashed line represents the linear regression of the standard curve (y = -3.409x + 37.479) with R2 = 0.999 and P <0.001.

277x152mm (96 x 96 DPI)

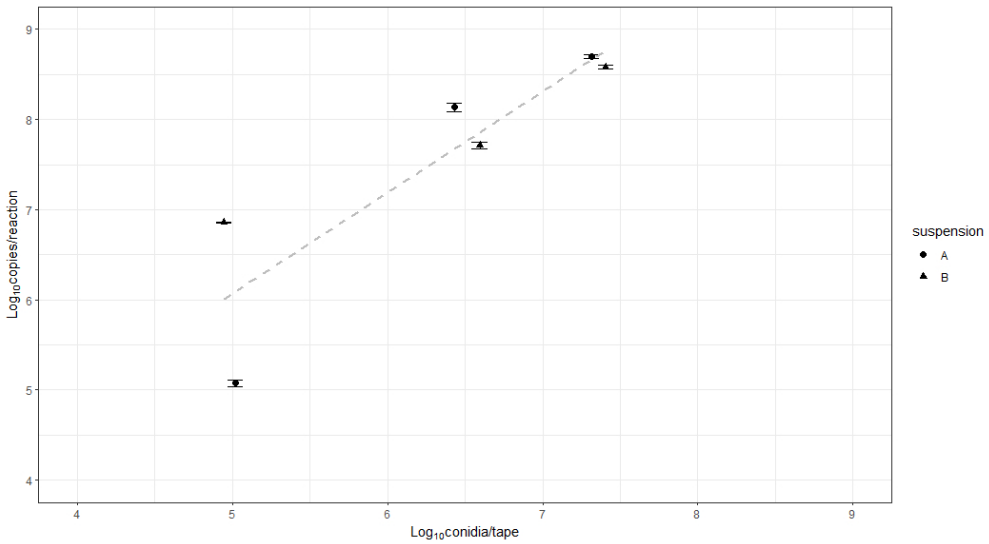

Fig. 3. Relationship between conidia counts obtained using light microscopy from conidial suspension series A and B and DNA copy number of Phaeomoniella chlamydospora. Conidia were counted in suspensions using a haemocytometer and a microscope. The suspensions were then added to tapes before DNA was extracted and subjected to qPCR for determination of DNA copy number. Values are means + SE of four replicates. The grey dashed line represents the linear regression model fit to the data (y = 0.808x + 2.679) with R2 = 0.729 and P = 0.019.

277x152mm (96 x 96 DPI)

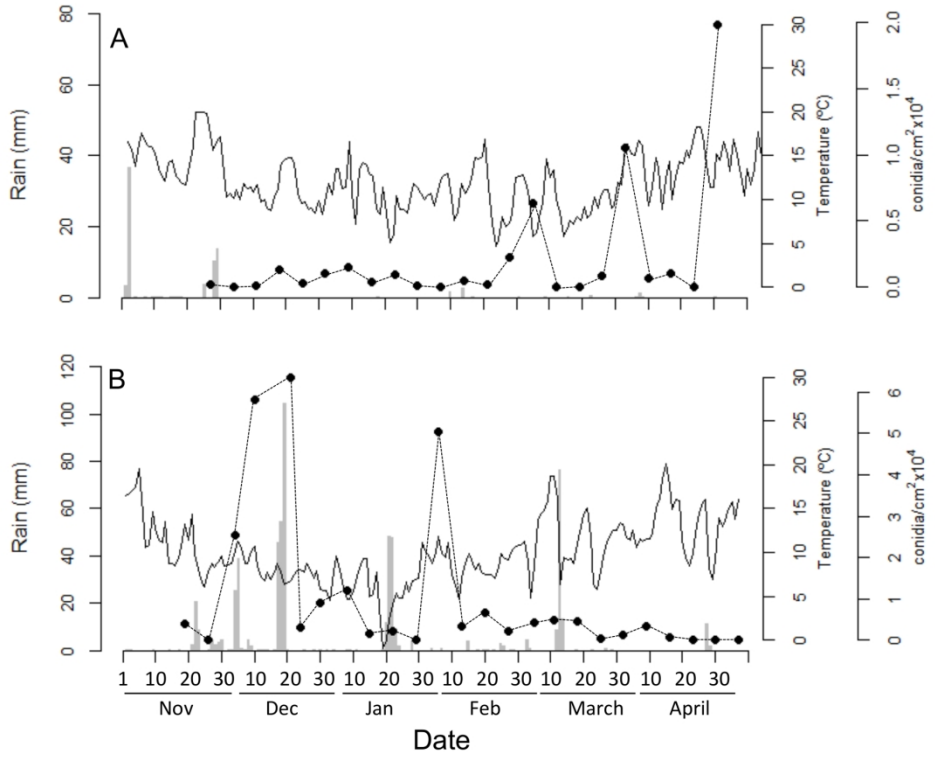

Fig. 4. Phaeomoniella chlamydospora inoculum detected on microscope slide traps in two vineyards in Ontinyent, Spain, in seasons 2015/2016 (A) and 2016/2017 (B). Black dots indicate the inoculum expressed as the average number of conidia/cm2 on five traps replaced weekly. The black line and grey bars represent the daily average temperature and the daily accumulated rain, respectively.

177x150mm (300 x 300 DPI)

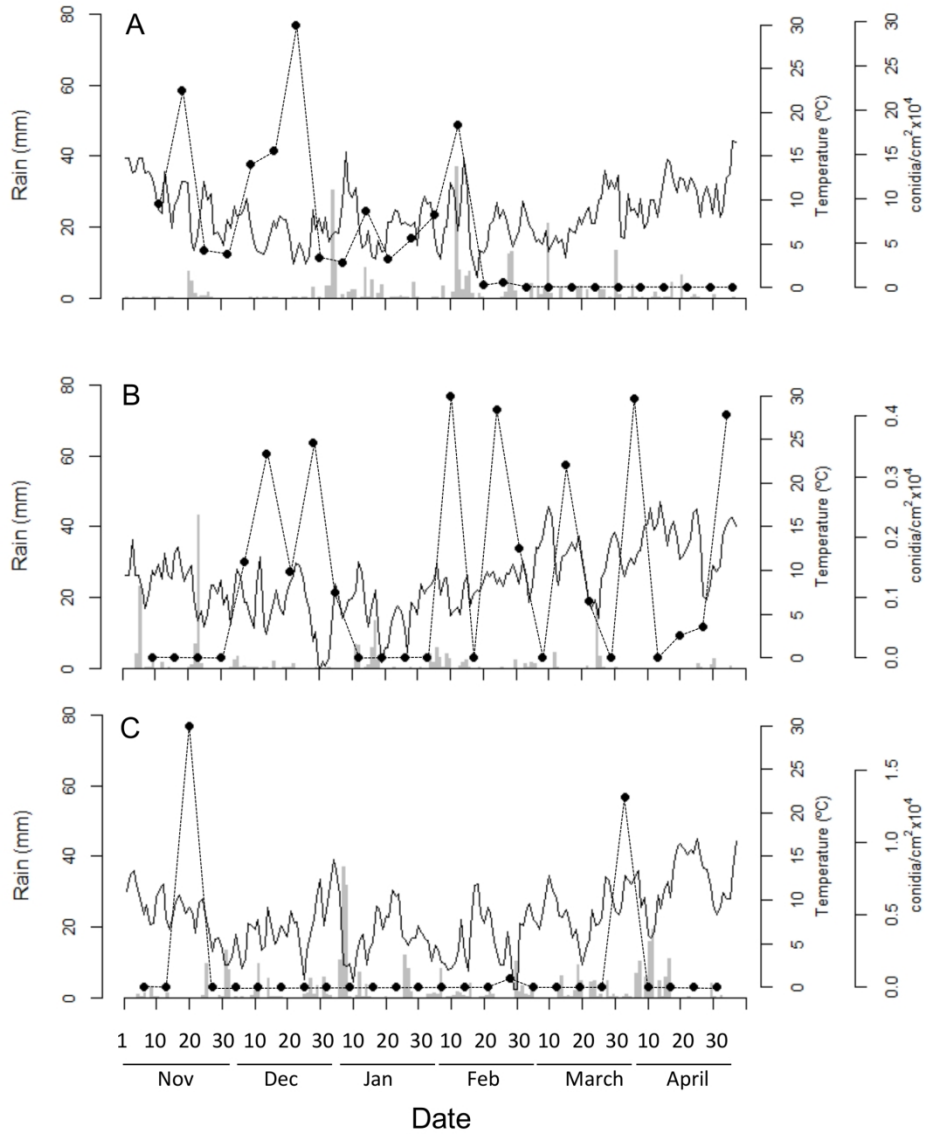

Fig. 5. Phaeomoniella chlamydospora inoculum detected in microscope slide traps in two vineyards in Logroño, Spain, in seasons 2015/2016 (A), 2016/2017 (B), and 2017/2018 (C). Black dots indicate the inoculum expressed as the average number of conidia/cm2 on five traps replaced weekly. The black line and grey bars represent the daily average temperature and the daily accumulated rain, respectively.

177x217mm (300 x 300 DPI)

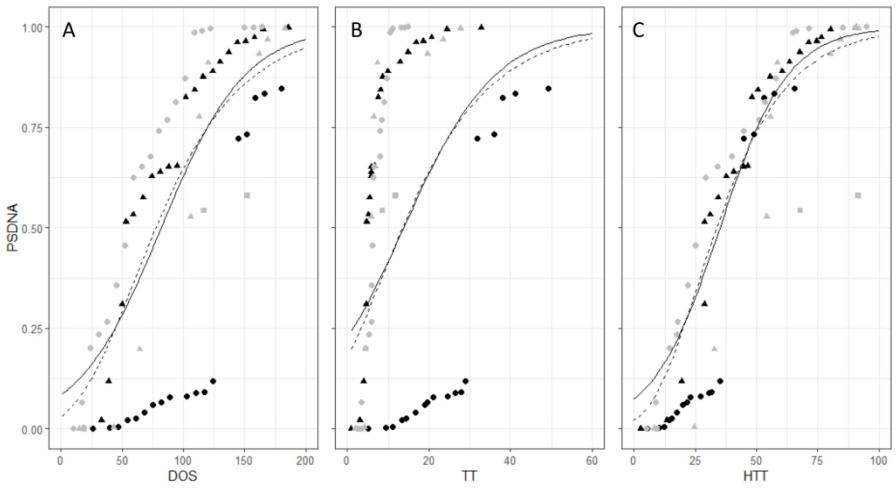

Proportion of the total seasonal inoculum (PSDNA) of Phaeomoniella chlamydospora detected over time on microscope slide traps in vineyards in 2015/2016 (dots), 2016/2017 (triangles), and 2017/2018 (squares): black and grey symbols indicate vineyards located in Ontinyent and Logroño, respectively. Time is expressed as day of the year starting on 1 November (DOS, A), thermal time (TT, B) or hydro-thermal time (HTT, C). Logistic (solid line) and Gompertz (dotted line) equations were fit to the data (Table 3).

275x190mm (300 x 300 DPI)

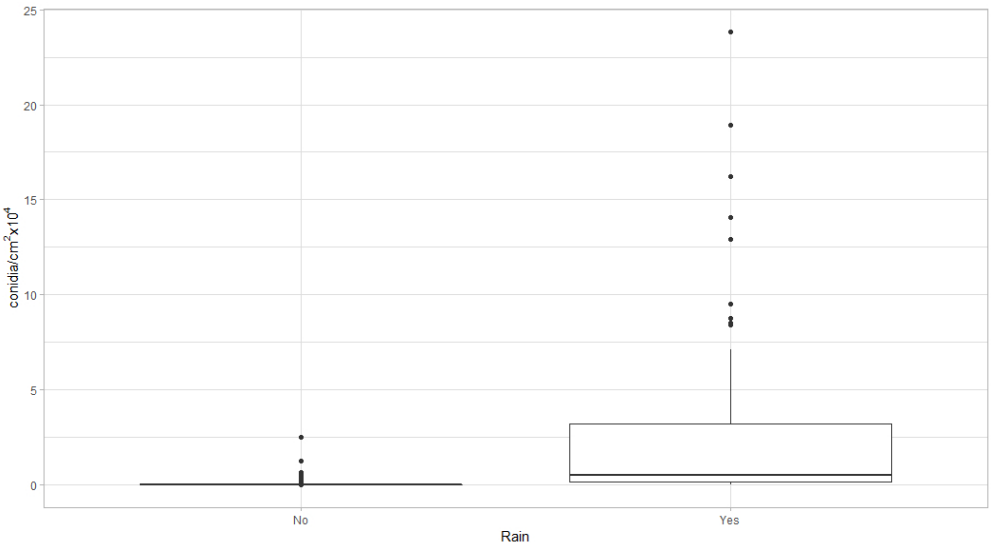

Fig. 7. Boxplots of the distributions of the DNA of Phaeomoniella chlamydospora detected on microscope slide traps in weeks without rain (n=72) or with rain (n=74). qPCR was used to detect and quantify the inoculum, which is expressed as the average number of conidia/cm2 on five traps replaced weekly. Boxes include the 2nd and 3rd quartiles; the thick black line is the median; whiskers extend to minimum and maximum values; and the dots are the outliers.

277x152mm (96 x 96 DPI)

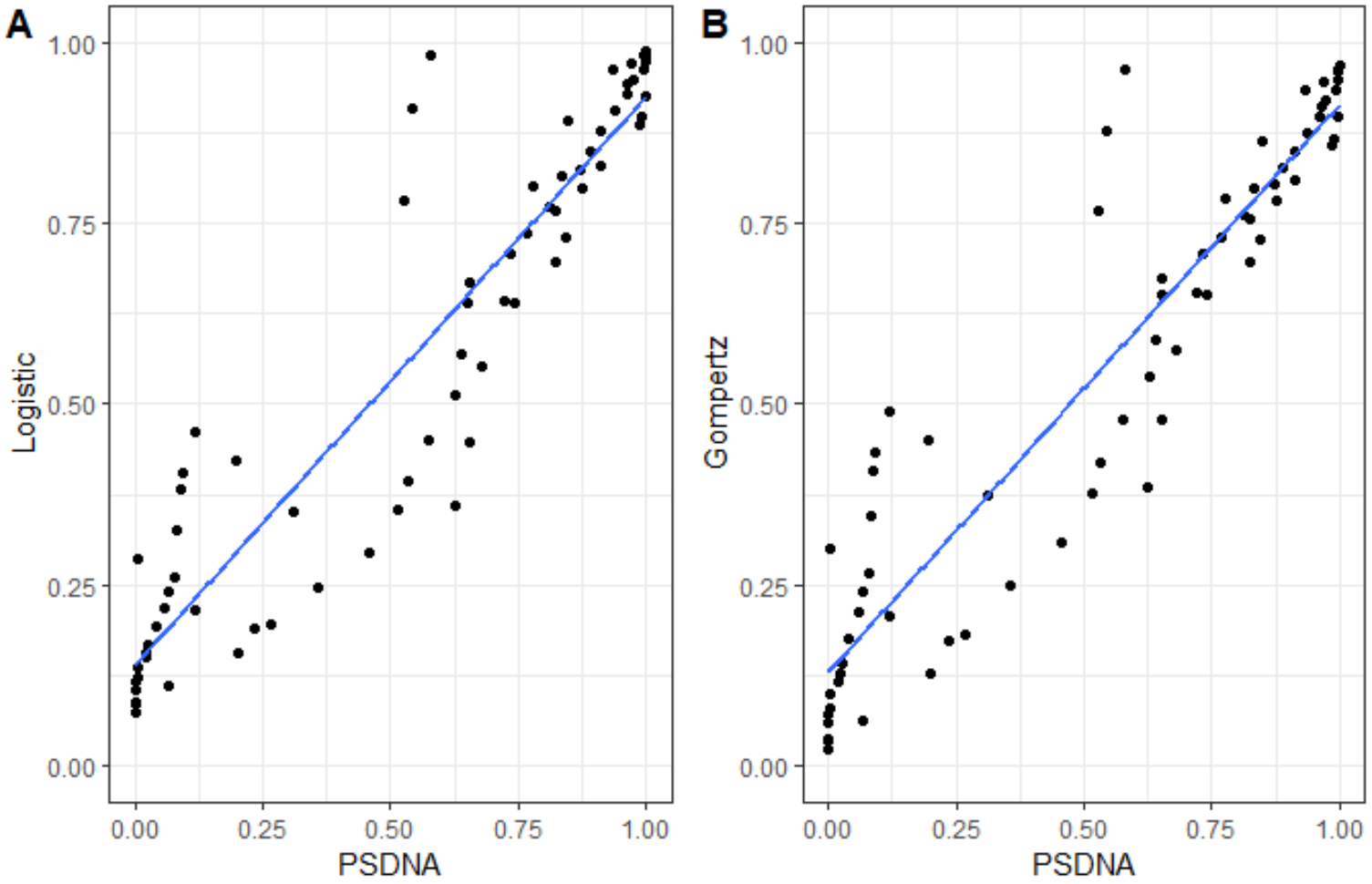

Figure S1. Observed versus predicted data on proportion of the total seasonal DNA (PSDNA) of *Phaeomoniella chlamydospora.* The inoculum was detected on microscope slide traps in Ontinyent (Spain) in 2015/2016 and 2016/2017 and in Logroño (Spain) in 2015/2016, 2016/2017 and 2017/2018. Data are predicted by a logistic (A) or a Gompertz equation (B). Parameters and goodness-of-fit indexes of the equations are described in Table 3.